optica

Spectroscopic detection of radiocarbon dioxide at parts-per-quadrillion sensitivity

Iacopo Galli,[1,2] Saverio Bartalini,[1,2] Riccardo Ballerini,[2] Marco Barucci,[3] Pablo Cancio,[1,2] Marco De Pas,[2] Giovanni Giusfredi,[1,2] Davide Mazzotti,[1,2,*] Naota Akikusa,[4] and Paolo De Natale[1,2]

[1]Istituto Nazionale di Ottica (INO)—CNR, Via Carrara 1, 50019 Sesto Fiorentino FI, Italy
[2]European Laboratory for Nonlinear Spectroscopy (LENS), Via Carrara 1, 50019 Sesto Fiorentino FI, Italy
[3]Istituto Nazionale di Ottica (INO)—CNR, Largo Fermi 6, 50125 Firenze FI, Italy
[4]Development Bureau Laser Device R&D Group, Hamamatsu Photonics KK, Shizuoka 434-8601, Japan
*Corresponding author: davide.mazzotti@ino.it

Received 18 December 2015; revised 5 February 2016; accepted 8 February 2016 (Doc. ID 255964); published 6 April 2016

High-sensitivity radiocarbon detection has been, until now, a prerogative of accelerator mass spectrometry (AMS). Here we present a compact and simple spectroscopic apparatus, based on saturated-absorption cavity ring-down, approaching the ultimate AMS sensitivity. We measure radiocarbon dioxide concentration down to a few parts per quadrillion by use of a heterodyne-spectroscopy system with two quantum cascade lasers at 4.5 μm, a reference cell, and a high-finesse cavity with the sample gas cooled down to 170 K. Our results pave the way to a paradigm change in radiocarbon measurement, with a number of significant applications in areas such as environment, nuclear security, pharmacology, and cultural heritage.

OCIS codes: (140.5965) Semiconductor lasers, quantum cascade; (280.3420) Laser sensors; (300.6390) Spectroscopy, molecular; (300.6340) Spectroscopy, infrared; (300.6360) Spectroscopy, laser; (300.6460) Spectroscopy, saturation.

http://dx.doi.org/10.1364/OPTICA.3.000385

The discovery of the radiocarbon dating method [1] has provided an unprecedented tool to assess the age of any sample of biological origin, in many different fields of knowledge (history, cultural heritage, forensic investigation, etc.). Since the late 1970s, accelerator mass spectrometry (AMS) has been, in fact, the benchmark for radiocarbon measurement, achieving parts-per-quadrillion (ppq, i.e., parts in 10^{-15}) $^{14}C/^{12}C$ detection sensitivity [2–4]. However, the best performing AMS instruments amount to only a few large, expensive facilities around the world, with high operation costs, mainly due to the management of very high voltages under ultrahigh vacuum. Aiming at a reduction of costs and at a wider spreading for less demanding applications, in recent years more and more compact AMS instruments have been developed [5,6] operating at lower and lower voltages, even without acceleration stages [7], recently reporting measurement precision as good as 0.2% for present-day natural abundance radiocarbon samples (currently named modern samples) [8].

A few years ago, the first optical detection of a radiocarbon-containing species was demonstrated by our group [9–13] with a proof-of-principle experiment based on the newly developed saturated-absorption cavity ring-down (SCAR) spectroscopic technique [14–18]. More recently, at least two other groups have reported radiocarbon dioxide detection with spectroscopic setups based on conventional cavity ring-down performed with quantum cascade lasers (QCLs), though achieving much worse results for the $^{14}C/C$ measurement, with detection limits ranging from 50 parts per trillion (ppt, i.e., parts in 10^{-12}) [19] to 4 ppt [20].

In this Letter, we show that radiocarbon dioxide concentration can be measured down to a few ppq by using an improved SCAR setup that has better performance, despite being simpler and less expensive.

A scheme of the experimental setup is shown in Fig. 1. With respect to the system presented in our previous works [9,10,13,15] (named SCAR1 in the following), the new setup (named SCAR2) relies on significant changes aimed, on the one hand, to improve the performance in terms of sensitivity, acquisition time, and amount of carbon sample needed, and, on the other hand, to drastically reduce the costs, power consumption, and size of the final instrument, thus envisaging a future portability.

The ring-down cavity has been redesigned from scratch, with several important new features. It can be cooled down to 170 K by means of a cryogen-free Stirling acoustic cryocooler (Qdrive, mod. 2S102K-FAR-DE-TI), instead of the "dry-ice bath" method used for the previous SCAR1 setup. The cavity is housed inside a vacuum chamber and wrapped in a multilayer aluminized-mylar super-insulation coat, thus strongly suppressing any convective and radiative heat transfer. With these technical measures, the overall thermal load coming from the outer environment is reduced at the level of about 3 W, and temperature differences along the cavity are lower than 1 K. This cooling system allows us to further reduce the effects of interfering hot-band lines from all other CO_2 isotopologues, especially the $(05^51 - 05^50)$ P(19)e transition of $^{13}C^{16}O_2$ at 2209.1159 cm^{-1}. Its volume has been reduced by about one order of magnitude, consequently lowering the amount of sample gas that is needed for the measurement

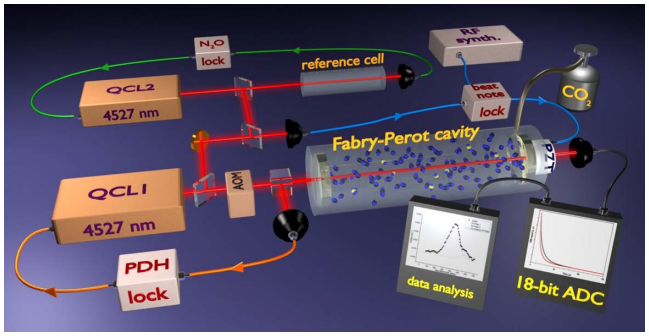

Fig. 1. Schematic of the experimental setup.

(corresponding to about 6 mg carbon content). Thanks to the improvement of the mirrors' reflectivity, with an unchanged cavity length (1 m), the effective interaction path is about 5.2 km, 40% longer than in SCAR1. The ZnSe mirrors have a multilayer dielectric coating with transmission $T = 87$ ppm and (absorption + scattering) $A = 103$ ppm, totaling overall losses $1 - R = 190$ ppm. Furthermore, a smaller radius of curvature (3 m instead of 6 m) produces a narrower beam waist of the TEM_{00} mode, thus enhancing the nonlinear saturation effects exploited by the SCAR technique. The longer decay time constant (17.5 μs instead of 12.5 μs) allows a more accurate sampling of the cavity ring-down signal, but also implies a longer acquisition time for each decay event (150 μs instead of 100 μs). This aspect is largely compensated by a more efficient management of the acquisition process, enabled by the new lock chain between the lasers and the cavity (see below). Indeed SCAR2 achieves an acquisition rate of about 2500 decays/s, more than double that of SCAR1.

The laser system has been completely changed with respect to SCAR1. SCAR2 employs two QCLs, both emitting in the range of 2208–2212 cm^{-1}, with output powers as large as 100 mW. QCL1 is used as a probe laser for the SCAR spectroscopy of the $(00^01 - 00^00)$ P(20) transition of $^{14}C^{16}O_2$, thus replacing the bulky intra-cavity source [21]. QCL2 is frequency-locked to the $(02^01 - 02^00)$ R(16)e transition of N_2O at 2209.0854 cm^{-1}. The first derivative of the absorption profile of this N_2O line is detected with the wavelength modulation spectroscopy technique, at a 5 mbar pressure and 12 cm absorption path-length. Hence, QCL2 plays a role that is analogous to the optical frequency comb synthesizer in SCAR1, providing a stable frequency reference around the targeted radiocarbon dioxide transition. The new laser system employs a frequency stabilization chain with two locking loops for efficiently narrowing and controlling the QCL1 frequency. First, QCL1 is frequency-locked to the high-finesse cavity by the Pound–Drever–Hall (PDH) technique. To this purpose, the QCL1 driving current is modulated at 4 MHz. A commercial phase-detector (Mini-Circuits, mod. ZRPD-1+) demodulates the error signal carried by the light fraction reflected back from the cavity and detected by a HgCdTe photodiode. This signal, conveniently processed and amplified by proportional/integral (PI) circuitry, is fed back to the laser current driver, achieving a locking bandwidth of about 300 kHz. In this way, the QCL1 linewidth is made narrower than the cavity resonance width (which is about 9 kHz), and its drift/jitter frequency fluctuations follow those of the cavity. Second, to achieve long-term stability of the QCL1 frequency, we control the cavity length by locking it to a stable reference, in particular the N_2O-locked QCL1. To this aim, the beatnote between QCL1 and QCL2 is detected by a fast (700 MHz bandwidth) HgCdTe photodiode. This beatnote is mixed with a stable local oscillator (RF synthesizer), and frequency fluctuations between the two lasers are retrieved by a home-made phase/frequency detector. After processing the error signal with another PI circuitry, the correction is fed back to the PZT moving one cavity mirror, with a locking bandwidth of about 500 Hz. Hence, thanks to this locking chain, the cavity-narrowed QCL1 absolute frequency is traceable to a molecular transition. Moreover, by tuning the frequency of the RF synthesizer, the cavity length is scanned and, consequently, the QCL1 absolute frequency, too, is scanned across the $^{14}C^{16}O_2$ target line profile.

Relative to the incoming optical power, about 54% is coupled to the cavity and about 16% is transmitted through it (corresponding to about 6 mW). These two measured values allow us to estimate the splitting of mirror losses between T and A (whose values are reported above) and the mode-matching efficiency, which results to be about 77%. The ring-down signal, detected by an InSb photodiode, is digitized by an 18-bit, 10 Msample/s analog-to-digital converter (ADC), and processed by real-time fitting software. An acousto-optic modulator (AOM), triggered by the ADC signal, is used to switch the light off at a given cavity-filling threshold, thus starting the cavity ring-down events.

A LabVIEW program controls all the experimental parameters and the acquisition routine, which has been optimized as the best trade-off between speed and sensitivity. A single acquisition consists of three back-and-forth stepwise scans of the QCL1 frequency across the target transition. For each frequency step, 3350 SCAR signals are acquired and averaged. A typical back-and-forth scan spans 600 MHz, with 61 points spaced by 10 MHz, and takes about 3.5 min.

The acquired SCAR decays for each scanned frequency are analyzed with the effective saturation parameter, Z_{1V}, a procedure thoroughly described in Ref. [16]. The value of Z_{1V} for a CO_2 sample at the present thermodynamic conditions (170 K and 12 mbar) is extrapolated from that measured at 195 K and 11.6 mbar [9,10,13]. As a result, the gas-induced cavity decay rate, γ_g, is determined for each scanned frequency. The six γ_g values belonging to the single sweeps (three back and three forth) are further averaged together. This procedure is performed in real time during the laser scan, and it actually does not increase the acquisition time.

Figure 2 shows the SCAR spectrum for a modern CO_2 sample averaged over a single measurement run made of three scans. The whole acquisition time for this spectrum is about 11 min. As expected at this temperature, the $(05^51 - 05^50)$ P(19)e transition of $^{13}C^{16}O_2$ at 2209.1159 cm^{-1}, which was the strongest interference absorption in previous experiments [9,10,13], is now almost totally suppressed. On the contrary, a weaker absorption from the N_2O molecule at almost the same frequency (i.e., the $(01^11 - 01^10)$ Q(12)e transition of $^{14}N_2^{16}O$ at 2209.1144 cm^{-1}) is now the strongest interference within the scanned frequency range. A comparable, or even better, S/N ratio for the detected spectrum can be noted with respect to previous results [9,13] but in a much shorter acquisition time, thus highlighting the improved performance of the present SCAR2 apparatus for real radiocarbon detection applications.

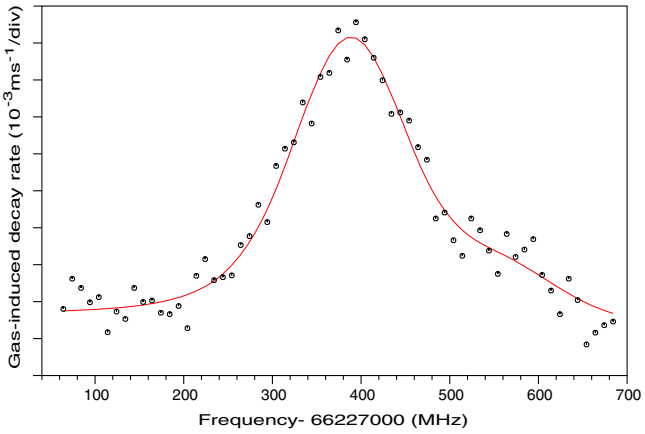

Fig. 2. SCAR spectrum measurement (with 11 min averaging time) of the ($00^01 - 00^00$) P(20) transition of $^{14}C^{16}O_2$ at 2209.1077 cm^{-1}, fitted together with the ($01^11 - 01^10$) Q(12)e interfering transition of $^{14}N_2^{16}O$ at 2209.1144 cm^{-1}.

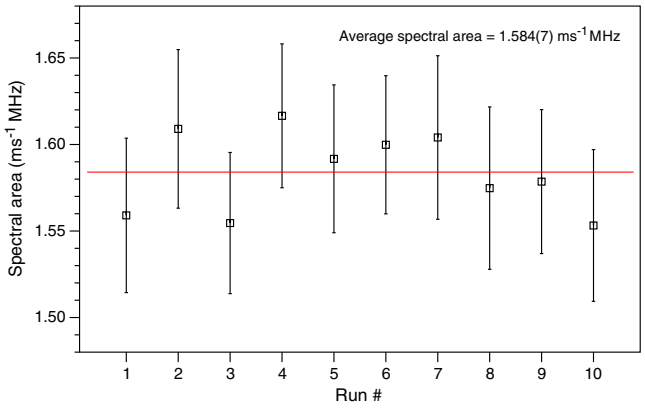

Fig. 3. Average spectral area measured over 10 runs.

In SCAR, radiocarbon dioxide concentrations are determined by measuring the spectral area of the absorption coefficient from the target P(20) transition of this molecule. To this aim, we fitted the measured SCAR spectrum to the expected absorption profile, as shown in Fig. 2. The fitting function takes into account, in an additive way, all absorbing molecular transitions lying within the scanned range. At the present sample temperature and pressure, a Voigt line shape is expected for both the P(20) and Q(12)e transitions of $^{14}C^{16}O_2$ and $^{14}N_2^{16}O$, respectively. Good agreement between experiment and fit can be noted. The spectral area of the P(20) line is determined with an uncertainty of about 3%, mainly limited by the S/N ratio and by the uncertainty in the spectral area of the interfering Q(12)e line. From this latter spectral area, we can estimate that the sample N_2O content was about 5 ppb, and we can conclude that a sample with even lower N_2O content is required to minimize any increase of the uncertainty budget for radiocarbon dioxide concentration measurements. It is worth noting that spectral area determinations with a lower uncertainty can be calculated by using a global line profile fitting procedure to analyze the recorded SCAR decays, as described in Ref. [16]. However, some molecular parameters, such as homogeneous and inhomogeneous linewidths and the saturation parameter at resonance, that are set in this fitting procedure as fixed constraints must be well calibrated for both transitions, considering the specific apparatus and the actual sample thermodynamic conditions to produce accurate results.

In order to analyze the repeatability and precision of the measured spectral areas and how they affect the final uncertainty in the radiocarbon dioxide concentration, we have recorded several 11-min-long runs by resetting for each run the experimental conditions, and by measuring the P(20) spectral area for each recording following the procedure described above. The result is shown in Fig. 3 for 10 runs. Repeatability comparable to the single run uncertainty allows a further precision improvement for the area determination, achieving a value of about 0.4% by weighted averaging of 10 consecutive runs, acquired in about 2 h. We are confident that averaging a larger number of runs could further improve precision at the cost of a longer acquisition time, which can be acceptable for some specific applications.

From the uncertainty quoted for the average area of Fig. 3, we can estimate a precision of about 5 ppq in 2 h for radiocarbon dioxide concentration determinations by using our current SCAR2 setup. The measured concentration also depends on the pressure and temperature of the sample gas, but their uncertainties, each amounting to less than 0.1%, are negligible at the present level of precision. Likewise, the uncertainty due to a possible calibration factor needed to get accurate values for the measured spectral area can also be considered negligible, as was demonstrated for the SCAR1 apparatus [16] (and SCAR2 is not expected to be different in this aspect). Otherwise, the estimated uncertainty for the line intensity at this temperature (0.5–1%) [22,23] cannot be considered completely negligible and would require either an improvement of the theoretical estimations or a direct measurement on a reference standard sample (like for AMS).

In conclusion, with the new SCAR2 setup we have shown a sensitivity improvement of more than one order of magnitude with respect to that achieved with our former SCAR1 setup [9,13]. Furthermore, it is worthwhile to discuss our results in view of specific applications. Carbon dioxide is a ubiquitous molecule, involved in metabolic and combustion processes; ^{14}C in particular is radioactive (with an half-life of 5700 years) and, as such, can only be detected in matter that is in equilibrium with the surrounding environment (or has been in equilibrium within timescales comparable with the half-life). Therefore, it is a key molecule for dating objects of biological origin (radiocarbon dating) or to discriminate between combustion of fossil fuels (totally depleted of ^{14}C) and bio-fuels [24–27]. It hence represents a marker for monitoring and discriminating carbon dioxide released in the atmosphere, with direct implications on climate change studies [28,29]. Finally, we remark that the SCAR technique is not limited to the detection of carbon dioxide, but can be applied to any molecule having sufficiently strong transitions to be saturable by available laser sources. This greatly widens the range of applicability of our technique, encompassing fields such as security, biomedicine, and environment, which can undergo a paradigmatic change from the proper exploitation of SCAR spectroscopy, which has pushed trace gas sensing much beyond the state of the art.

Funding. Programma Nazionale di Ricerche in Antartide (PNRA) (project 2013/AC4.01); ESFRI Roadmap Project

"Extreme Light Infrastructure (ELI); EU 7th Framework Program 284464.

Acknowledgment. We thank A. Montori and M. Giuntini for designing and building the detector front-end electronics.

REFERENCES

1. J. R. Arnold and W. F. Libby, Science **113**, 111 (1951).
2. A. E. Litherland, X.-L. Zhao, and W. E. Kieser, Mass Spectrom. Rev. **30**, 1037 (2011).
3. H.-A. Synal, Int. J. Mass Spectrom. **349–350**, 192 (2013).
4. W. Kutschera, Int. J. Mass Spectrom. **349–350**, 203 (2013).
5. H.-A. Synal, M. Stocker, and M. Suter, Nucl. Instrum. Methods Phys. Res. Sect. B **259**, 7 (2007).
6. T. Schulze-König, S. R. Dueker, J. Giacomo, M. Suter, J. S. Vogel, and H.-A. Synal, Nucl. Instrum. Methods Phys. Res. Sect. B **268**, 891 (2010).
7. H.-A. Synal, T. Schulze-König, M. Seiler, M. Suter, and L. Wacker, Nucl. Instrum. Methods Phys. Res. Sect. B **294**, 349 (2013).
8. E. Bard, T. Tuna, Y. Fagault, L. Bonvalot, L. Wacker, S. Fahrni, and H.-A. Synal, Nucl. Instrum. Methods Phys. Res. Sect. B **361**, 80 (2015).
9. I. Galli, S. Bartalini, S. Borri, P. Cancio, D. Mazzotti, P. De Natale, and G. Giusfredi, Phys. Rev. Lett. **107**, 270802 (2011).
10. I. Galli, P. Cancio, G. Di Lonardo, L. Fusina, G. Giusfredi, D. Mazzotti, F. Tamassia, and P. De Natale, Mol. Phys. **109**, 2267 (2011).
11. D. Mazzotti, S. Bartalini, S. Borri, P. Cancio, I. Galli, G. Giusfredi, and P. De Natale, Opt. Photon. News **23**(12), 52 (2012).
12. R. N. Zare, Nature **482**, 312 (2012).
13. I. Galli, S. Bartalini, P. Cancio, P. De Natale, D. Mazzotti, G. Giusfredi, M. E. Fedi, and P. A. Mandò, Radiocarbon **55**, 213 (2013).
14. G. Giusfredi, S. Bartalini, S. Borri, P. Cancio, I. Galli, D. Mazzotti, and P. De Natale, Phys. Rev. Lett. **104**, 110801 (2010).
15. P. Cancio, S. Bartalini, S. Borri, I. Galli, G. Gagliardi, G. Giusfredi, P. Maddaloni, P. Malara, D. Mazzotti, and P. De Natale, Appl. Phys. B **102**, 255 (2011).
16. G. Giusfredi, I. Galli, D. Mazzotti, P. Cancio, and P. De Natale, J. Opt. Soc. Am. B **32**, 2223 (2015).
17. G. Giusfredi, I. Galli, P. Cancio, D. Mazzotti, and P. De Natale, "Apparatus and method for measuring the concentration of trace gases by SCAR spectroscopy," PCT Application WO/2014/170828 (October 23, 2014).
18. P. Cancio, P. De Natale, I. Galli, G. Giusfredi, and D. Mazzotti, "Apparato per la misura di concentrazione di gas in tracce mediante la spettroscopia SCAR," Italian patent 0001417063 (October 16, 2014).
19. G. Genoud, M. Vainio, H. Phillips, J. Dean, and M. Merimaa, Opt. Lett. **40**, 1342 (2015).
20. A. D. McCartt, T. Ognibene, G. Bench, and K. Turteltaub, Nucl. Instrum. Methods Phys. Res. Sect. B **361**, 277 (2015).
21. I. Galli, S. Bartalini, S. Borri, P. Cancio, G. Giusfredi, D. Mazzotti, and P. De Natale, Opt. Lett. **35**, 3616 (2010).
22. O. L. Polyansky, K. Bielska, M. Ghysels, L. Lodi, N. F. Zobov, J. T. Hodges, and J. Tennyson, Phys. Rev. Lett. **114**, 243001 (2015).
23. J. Tennyson, Department of Physics and Astronomy, University College London, UK (Personal communication, 2015).
24. K. Hämäläinen, H. Jungner, O. Antson, J. Räsänen, K. Tormonen, and J. Roine, Radiocarbon **49**, 325 (2007).
25. J. Mohn, S. Szidat, J. Fellner, H. Rechberger, R. Quartier, B. Buchmann, and L. Emmenegger, Bioresour. Technol. **99**, 6471 (2008).
26. S. W. L. Palstra and H. A. J. Meijer, Radiocarbon **56**, 7 (2014).
27. F.-J. Santos Arévalo, I. Gómez Martínez, L. Agulló García, M. T. Reina Maldonado, and M. García León, Nucl. Instrum. Methods Phys. Res. Sect. B **361**, 354 (2015).
28. H. D. Graven and N. Gruber, Atmos. Chem. Phys. **11**, 12339 (2011).
29. S. Lehman, J. Miller, C. Wolak, J. Southon, P. Tans, S. Montzka, C. Sweeney, A. Andrews, B. LaFranchi, T. Guilderson, and J. Turnbull, Radiocarbon **55**, 1484 (2013).